

# $\alpha$ -MnO<sub>2</sub> Nanowires: A Catalyst for the O<sub>2</sub> Electrode in Rechargeable Lithium Batteries\*\*

Aur lie D bart, Allan J. Paterson, Jianli Bao, and Peter G. Bruce\*

Charge storage in rechargeable lithium batteries is limited by the positive electrode, usually the lithium intercalation compound LiCoO<sub>2</sub>, which can store 130 mA h g<sup>−1</sup>.<sup>[1–3]</sup> Intense efforts are underway worldwide to discover new lithium intercalation compounds for use as positive electrodes which, it is hoped, may deliver specific capacities of about 300 mA h g<sup>−1</sup>. However, increasing the capacity significantly beyond this limit is a major challenge requiring a more radical approach, such as replacement of the intercalation electrode by an O<sub>2</sub> electrode, in which Li<sup>+</sup> from the electrolyte and e<sup>−</sup> from the external circuit combine reversibly with O<sub>2</sub> from the air within a porous matrix containing a catalyst.<sup>[4–8]</sup> Although it provides higher capacities than intercalation electrodes, much fundamental work is required to understand and optimize the performance of the O<sub>2</sub> electrode for lithium batteries before it can be considered further for technological application. The nature of the catalyst plays a key role. It is important to identify good catalysts for the electrode reaction before focusing on other tasks, such as reducing the catalyst loading and optimizing porosity, binder, and electrolyte. Herein we show that  $\alpha$ -MnO<sub>2</sub> nanowires give the highest charge storage capacity yet reported for such an electrode, reaching 3000 mA h per gram of carbon, or 505 mA h g<sup>−1</sup> if normalized by the total electrode mass. Furthermore, by avoiding deep discharge, excellent capacity retention has been demonstrated. Finally, the capacities delivered by an O<sub>2</sub> electrode and a conventional intercalation compound are compared.

The reversible oxygen electrode is shown schematically in Figure 1. On discharge, the Li<sup>+</sup> ions (electrolyte) and e<sup>−</sup> (external circuit) combine with O<sub>2</sub> (air) to form Li<sub>2</sub>O<sub>2</sub> within the pores of the porous carbon electrode.<sup>[4–8]</sup> Previously, we demonstrated that rechargeability of the Li/O<sub>2</sub> cell involves decomposition of Li<sub>2</sub>O<sub>2</sub> back to Li and O<sub>2</sub>.<sup>[8]</sup> Our earlier studies on the rechargeable Li/O<sub>2</sub> cell focused on electrolytic manganese dioxide (EMD) as catalyst in the oxygen electrode.<sup>[8]</sup> Recently, we examined a number of other potential catalyst materials including Co<sub>3</sub>O<sub>4</sub>, Fe<sub>2</sub>O<sub>3</sub>, CuO, and CoFe<sub>2</sub>O<sub>4</sub>.<sup>[9]</sup> Such investigations served to demonstrate that the nature of the catalyst is a key factor controlling the

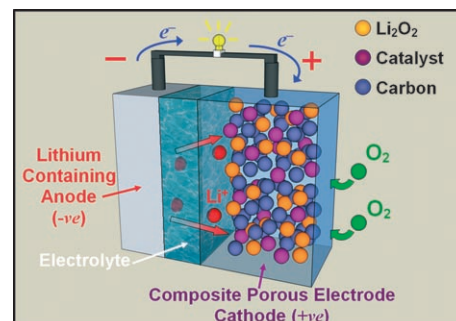


Figure 1. Schematic representation of a rechargeable Li/O<sub>2</sub> battery.

performance of the oxygen electrode, especially the capacity, which is the primary reason for interest in the O<sub>2</sub> electrode. Herein we report on the high capacities that an  $\alpha$ -MnO<sub>2</sub> nanowire catalyst can deliver. We also compare the performance of  $\alpha$ -MnO<sub>2</sub> with other manganese oxide compounds. Note that the specific capacities are normalized with respect to the mass of carbon in the electrode, as is usual for porous electrodes; this point is discussed at the end of the paper.

Synthesis and characterization of the various MnO<sub>x</sub> catalysts and their incorporation into lithium cells with porous electrodes is described in the *Experimental Section*. Powder X-ray diffraction data were collected for all catalysts (see the Supporting Information) and confirmed their identities ( $\alpha$ -MnO<sub>2</sub> in bulk and nanowire form,  $\beta$ -MnO<sub>2</sub> in bulk and nanowire form,  $\gamma$ -MnO<sub>2</sub>,  $\lambda$ -MnO<sub>2</sub>, Mn<sub>2</sub>O<sub>3</sub>, and Mn<sub>3</sub>O<sub>4</sub>).

The variation of capacity with cycle number for a porous electrode containing  $\alpha$ -MnO<sub>2</sub> nanowires as catalyst is presented in Figure 2a, from which the superior behavior of the  $\alpha$ -MnO<sub>2</sub> catalyst is evident. The initial discharge capacity is 3000 mA h g<sup>−1</sup>, it then drops slightly, rises again to 3100 mA h g<sup>−1</sup> on cycle 4, before declining steadily thereafter. This may be contrasted with previous reports for EMD, the capacity of which falls below 1000 mA h g<sup>−1</sup> after one cycle (Figure 2a).<sup>[8]</sup> The variation of potential with state of charge for several cycles of  $\alpha$ -MnO<sub>2</sub> is shown in Figure 2b. As observed previously for all other catalysts, the discharge voltage is around 2.6 V versus Li<sup>+</sup>/Li<sup>0</sup>.<sup>[8,9]</sup> Previous results have demonstrated that the charging potential varies according to the catalyst type.<sup>[9]</sup> Values ranging from 4 to 4.7 V versus Li<sup>+</sup>/Li<sup>0</sup> have been observed, and  $\alpha$ -MnO<sub>2</sub> exhibits a charging potential at the lower end of this spectrum, at around 4.0 V. This is another advantage of the  $\alpha$ -MnO<sub>2</sub> nanowires, since it is important to minimize the charging potential. Note that  $\alpha$ -MnO<sub>2</sub>, and many of the other MnO<sub>x</sub> compounds described herein, support some Li intercalation. However,

[\*] Dr. A. D bart, Dr. A. J. Paterson, J. Bao, Prof. P. G. Bruce  
Eastchem, School of Chemistry  
University of St Andrews  
St Andrews, KY16 9ST (UK)  
Fax: (+44) 1334-463-808  
E-mail: pgb1@st-andrews.ac.uk

[\*\*] P. G. B. is indebted to the EPSRC for financial support.

Supporting information for this article is available on the WWW under <http://www.angewandte.org> or from the author.

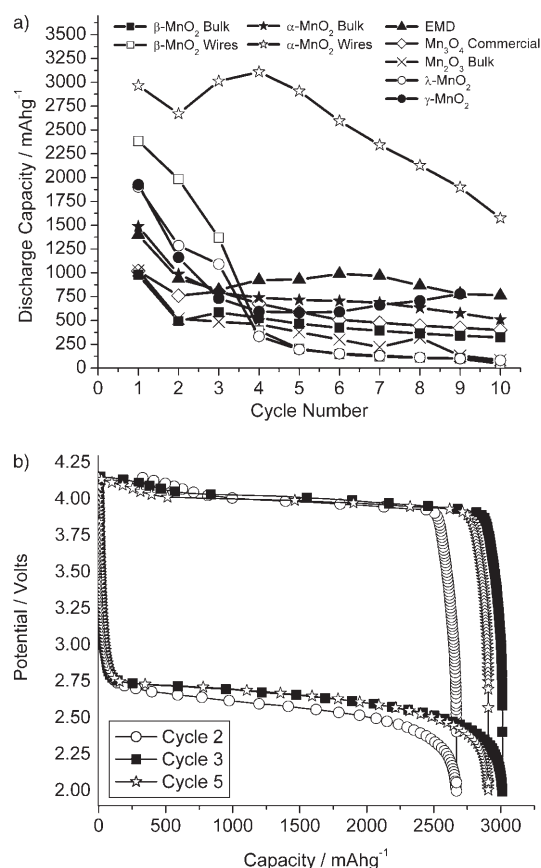


**Figure 2.** a) Variation of discharge capacity with cycle number for several porous electrodes containing manganese oxides as catalysts:  $\alpha$ - $\text{MnO}_2$  in bulk and nanowire form,  $\beta$ - $\text{MnO}_2$  in bulk and nanowire form,  $\gamma$ - $\text{MnO}_2$ ,  $\lambda$ - $\text{MnO}_2$ ,  $\text{Mn}_2\text{O}_3$ , and  $\text{Mn}_3\text{O}_4$ . EMD is included herein for comparison but was reported previously.<sup>[8]</sup> Cycling was carried out at a rate of  $70 \text{ mA g}^{-1}$  in 1 atm of  $\text{O}_2$ . Capacities are per gram of carbon in the electrode. Lower cutoff potential 2 V. b) Variation of potential with state of charge for the porous electrode containing  $\alpha$ - $\text{MnO}_2$  nanowires reported in Figure 2a, cycled at a rate of  $70 \text{ mA g}^{-1}$  between 2 and 4.15 V.

such intercalation could not explain the high capacities shown in Figure 2.

A cell containing  $\alpha$ - $\text{MnO}_2$  as catalyst was disassembled at the end of discharge, and the electrode investigated by Raman spectroscopy. The results (see the Supporting Information) confirmed that the dominant product of discharge was  $\text{Li}_2\text{O}_2$ , as observed previously for EMD.<sup>[8]</sup> Formation and decomposition of  $\text{Li}_2\text{O}_2$  on discharge and charge were followed by examining the electrode by scanning electron microscopy in different states of charge and discharge (see Figure S3 in the Supporting Information).

The performance of the  $\alpha$ - $\text{MnO}_2$  nanowires is compared with that of electrodes containing other manganese oxide catalysts in Figure 2a. The electrodes were constructed in an identical fashion to those containing the  $\alpha$ - $\text{MnO}_2$  nanowires and with the same proportion of carbon, catalyst, and binder. The other  $\text{MnO}_2$  polymorphs,  $\beta$ ,  $\gamma$  and  $\lambda$ , either exhibit lower capacities or capacities that fade very rapidly on cycling; their overall performance is markedly inferior to that of  $\alpha$ - $\text{MnO}_2$  nanowires. The performances of  $\text{Mn}_2\text{O}_3$  and the spinel  $\text{Mn}_3\text{O}_4$

are also inferior to that of  $\alpha$ - $\text{MnO}_2$  nanowires. This is also the case for non-manganese catalysts studied previously.<sup>[9]</sup>

Given the catalytic role of the manganese oxides, it is interesting to examine the effect of changing the surface area on the performance. An indication of this can be obtained by comparing the performance of  $\alpha$ - and  $\beta$ - $\text{MnO}_2$  catalysts prepared in bulk and nanowire form (Figure 2a). The morphologies are shown in Figure 3. The  $\alpha$ - $\text{MnO}_2$  nanowires

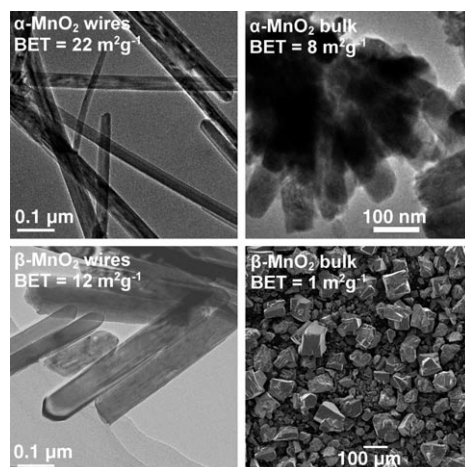


**Figure 3.** TEM/SEM images of bulk and nanowire forms of  $\alpha$ - and  $\beta$ - $\text{MnO}_2$  polymorphs showing their morphologies and surface areas.

are typically 30–40 nm in diameter and can be up to several 100 nm long. The corresponding bulk material also has an elongated morphology, although the aspect ratio is not as high as that of the nanowires, and typical dimensions are around 60–80 nm in diameter and 200–400 nm in length. From Figure 2a it is evident that the nanowires have much higher capacity than the bulk material. This improvement is also observed when comparing nanowire and bulk  $\beta$ - $\text{MnO}_2$  (Figure 3). Here the elongated nature of the structure is not preserved in the bulk material, and this suggests that the enhanced performance of the nanomaterials is due largely to their higher surface area rather than their morphology. However, it is also important to note that the surface area of the  $\alpha$ - and  $\beta$ - $\text{MnO}_2$  nanowires differs by less than a factor of two, yet the overall performance of the former on cycling is far superior to that of the latter, that is, the nature of the catalyst is the key, not just the surface area.

Although capacities in excess of  $3000 \text{ mA h g}^{-1}$  can be obtained by using  $\alpha$ - $\text{MnO}_2$  nanowires as catalyst, not only in the first cycle, it is evident from Figure 2 that the capacities of this and all other catalysts fade. Indeed capacity fading has been a feature of all previous results on such  $\text{O}_2$  electrodes.<sup>[4,5,8,9]</sup> This suggests that the origin of capacity fading does not lie with the type of catalyst. Voltage polarization occurs at the end of discharge (Figure 2b). If deep discharge is avoided by limiting the discharge capacity to values that avoid such polarization, excellent capacity retention can be obtained, as illustrated in Figure 4. We do not propose limiting the capacity as a technological solution to the problem of capacity fade, but rather as an indicator of the possible origin of fading.

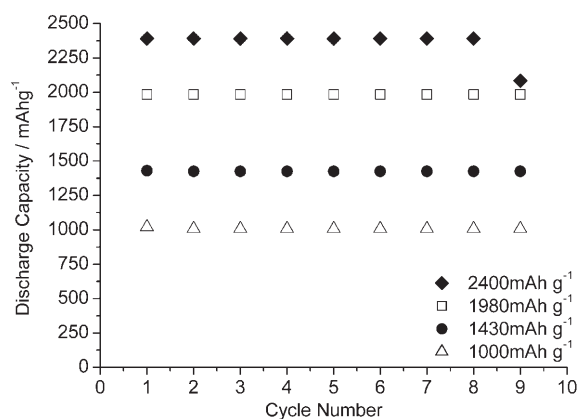


**Figure 4.** Variation of discharge capacity with cycle number for porous electrodes containing  $\alpha$ - $\text{MnO}_2$  nanowires as catalyst when the state of discharge is limited to different degrees. Cycling rate of  $70 \text{ mA g}^{-1}$ . Capacities per gram of carbon in the electrode.

Even at  $2400 \text{ mA h g}^{-1}$  there is some evidence of fade at the end of cycling. The key point is that avoiding polarization (deep discharge) leads to better cyclability. This may reflect the fact that the formation of a large amount of  $\text{Li}_2\text{O}_2$  in the pores at deep discharge results in their becoming blocked or causes expansion of the electrode leading to loss of contact between electrode particles during subsequent recharge. Such processes are not related to the nature of the catalyst per se and are therefore beyond the scope of this paper. However, work is ongoing to understand and hence minimize capacity fading (e.g., by controlling the electrode pore size/distribution). By better engineering the electrode it should be possible to increase the utilization and thus provide access to the capacities of about  $3000 \text{ mA h g}^{-1}$  that are already available for a few cycles.

Why does  $\alpha$ - $\text{MnO}_2$  perform better than other closely related manganese oxides? The crystal structure of the  $\alpha$  polymorph is that of hollandite and consists of  $2 \times 2$  tunnels formed by edge- and corner-sharing  $\text{MnO}_6$  octahedra.<sup>[10]</sup>  $\text{Li}_2\text{O}$  can be incorporated within the tunnels, with the  $\text{O}^{2-}$  ions located at the tunnel centers and the  $\text{Li}^+$  ions coordinated between these central  $\text{O}^{2-}$  ions and those forming the walls of the tunnels. The ability to accommodate both  $\text{Li}^+$  and  $\text{O}^{2-}$  within the tunnels suggests the possibility of incorporating  $\text{Li}^+$  and  $\text{O}_2^{2-}$ . Such incorporation is not possible in the other  $\text{MnO}_2$  polymorphs or indeed the other  $\text{MnO}_x$  materials. Since the major role of the catalyst is to promote the reversibility of  $\text{Li}_2\text{O}_2$  formation, it is tempting to relate these two features and suggest that the ability of the crystal structure to incorporate  $\text{Li}^+$  and  $\text{O}^{2-}$ , most likely near the surface of the material, is pertinent to the good performance of this catalyst. However, identifying  $\text{Li}_2\text{O}_2$  in the near-surface regions of  $\alpha$ - $\text{MnO}_2$  will be a considerable challenge.

Porous gas electrodes are not new; they are ubiquitous in fuel cells, and aqueous batteries containing air cathodes, for example,  $\text{Zn/air}$  and  $\text{Fe/air}$ , have been known for sometime. In reporting the behavior of air electrodes, the convention of normalizing the capacity with respect to the mass of carbon has been used for some years, a convention that has been adhered to herein. Reasons for the convention are that carbon

is the dominant component of the porous electrode and the electrode mass increases as discharge proceeds, due to accumulation of  $\text{Li}_2\text{O}_2$  in the electrode. However, the simplicity of this convention somewhat obscures a direct comparison of the specific capacity of an  $\text{O}_2$  electrode with that of an intercalation cathode. The total mass of the cathode at the end of discharge (carbon + binder + catalyst +  $\text{Li}_2\text{O}_2$ ) can be used to calculate the specific capacity. However, ultimately it is the contribution to the capacity of the whole battery that matters, and including  $\text{Li}_2\text{O}_2$  overestimates the mass gained during discharge, since only the mass of  $\text{O}_2$  is added to the cell; the Li, which comes from the anode, would be counted twice (The mass of Li is not included in calculating the specific capacity of  $\text{V}_2\text{O}_5$ , for example). Even allowing for this correction, the use of total cathode mass plus  $\text{O}_2$  gained is only strictly relevant at the deepest discharge.

Figure 5 shows the specific capacity for the  $\alpha$ - $\text{MnO}_2$  nanowires based on total electrode mass at the beginning and end of discharge. Converting the capacity of

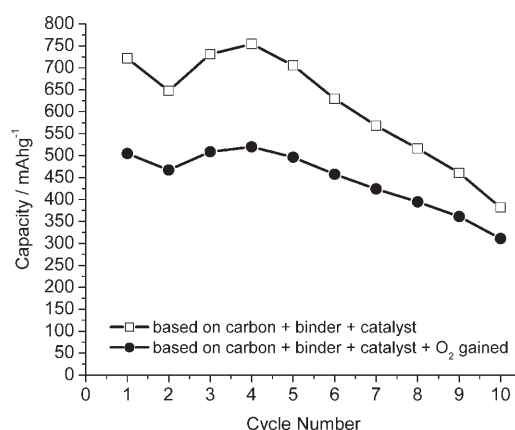


**Figure 5.** Variation of discharge capacity with cycle number for porous electrodes containing  $\alpha$ - $\text{MnO}_2$  nanowires as catalyst, based on total electrode mass at the beginning (carbon + binder + catalyst) and end (carbon + binder + catalyst +  $\text{O}_2$ ) of discharge.

$3000 \text{ mA h g}^{-1}$  (carbon) into the specific capacities based on the total masses gives  $730 \text{ mA h g}^{-1}$  (carbon + binder + catalyst) and  $505 \text{ mA h g}^{-1}$  (carbon + binder + catalyst +  $\text{O}_2$ ). For the restricted capacity cycling shown in Figure 4, the specific capacity of  $2400 \text{ mA h g}^{-1}$  (carbon) would correspond to  $540 \text{ mA h g}^{-1}$  (carbon + binder + catalyst) and  $408 \text{ mA h g}^{-1}$  (carbon + binder + catalyst +  $\text{O}_2$ ). Since in the case of intercalation electrodes only the mass of active material is usually employed to calculate specific capacities, comparison requires addition of the mass of carbon and binder to normalize the charge passed. For a typical mass ratio in a composite cathode containing an intercalation compound of 85:10:5 (active material:carbon:binder), the specific capacities for  $\text{LiCoO}_2$ ,  $\text{LiCo}_{1/3}\text{Mn}_{1/3}\text{Ni}_{1/3}\text{O}_2$ ,  $\text{LiMn}_2\text{O}_4$  and  $\text{LiFePO}_4$ , based on the total mass, would be 111, 170, 102, and  $132 \text{ mA h g}^{-1}$ , respectively. Clearly, the capacities of the  $\text{O}_2$  cathode far exceed these values.

The focus of the present paper is the performance of the different manganese oxides as catalysts in the  $\text{O}_2$  electrode. To

facilitate comparison between the different catalysts the proportions of carbon:catalyst:binder were fixed. However, if the dimensions of the  $\alpha$ -MnO<sub>2</sub> nanowires were reduced to a diameter and length of 10 and 200 nm, respectively, the loading (mass of catalyst in the electrode) could be reduced by 72 % while maintaining the same surface area, and specific capacities of 1076 (carbon + binder + catalyst) and 655 mA h g<sup>-1</sup> (carbon + binder + catalyst + O<sub>2</sub>) would result.

An estimate of the maximum capacity that can be expected from an O<sub>2</sub> electrode can be made. If we assume a carbon cathode with a porosity of 75 % (such porosity should still ensure electron percolation through the carbon matrix) and use Li<sub>2</sub>O<sub>2</sub> formation as the basis but consider the mass gain to be only O<sub>2</sub>, a value of 1220 mA h g<sup>-1</sup> is obtained. This of course does not allow for the mass of binder or catalyst, and therefore in practice values will be lower. However, it emphasizes that, having identified an optimum catalyst, the next stage must be to minimize the proportions of catalyst and binder.

In summary, the data presented herein show that the use of  $\alpha$ -MnO<sub>2</sub> nanowires as catalyst in an oxygen cathode for rechargeable lithium batteries can deliver capacities of 3000 mA h g<sup>-1</sup> of carbon or 730 and 505 mA h g<sup>-1</sup> based on total electrode masses excluding and including O<sub>2</sub>, respectively. These values significantly exceed those of conventional cathodes for rechargeable lithium batteries. By restricting the depth of discharge, it is possible to obtain good capacity retention on cycling, that is, cyclability is not limited by the catalyst but more likely by the porosity of the electrode. Identifying a good catalyst is the necessary first step in optimizing the performance. Having done so, future work will be directed to reducing the loading of catalyst and thus minimizing the total mass of the electrode. Such optimized electrode construction is akin to work on fuel cells, which has seen a reduction in particle size and loading of catalyst, although in that case a major driver is the high cost of Pt rather than the mass of the electrode.

The O<sub>2</sub> electrode is not an immediate technological solution for high-capacity rechargeable lithium batteries. Issues such as a membrane to protect the cathode from ingress of CO<sub>2</sub>/H<sub>2</sub>O, an optimized electrolyte, safety testing, and extended cycling, must be addressed. However, the capacities reported herein, which exceed those of conventional rechargeable intercalation battery cathodes such as LiCoO<sub>2</sub>, LiFePO<sub>4</sub>, and Li(Co<sub>1/3</sub>Ni<sub>1/3</sub>Mn<sub>1/3</sub>)O<sub>2</sub>, encourage further investigation of the O<sub>2</sub> electrode.

### Experimental Section

Synthesis and characterization of various MnO<sub>x</sub> catalysts: Bulk Mn<sub>2</sub>O<sub>3</sub> and Mn<sub>3</sub>O<sub>4</sub> were obtained from Aldrich, and bulk  $\beta$ -MnO<sub>2</sub> from Strem. All other MnO<sub>2</sub> catalysts—bulk and nanowire  $\alpha$ -MnO<sub>2</sub>, nanowire  $\beta$ -MnO<sub>2</sub>, bulk  $\gamma$ -MnO<sub>2</sub>, and bulk  $\lambda$ -MnO<sub>2</sub>—were prepared according to literature procedures.<sup>[11–15]</sup>

Powder X-ray diffraction data were collected for all the catalysts on a STOE STADI/P diffractometer operating with FeK $\alpha$  radiation ( $\lambda = 1.936$  Å). Surface areas were determined by N<sub>2</sub> adsorption/desorption (Micrometrics ASAP2020), and morphologies were examined by SEM (JEOL JSM-5600 and FEI quanta 200F) and TEM (JEOL 2010).

Electrochemical measurements: Electrochemical cycling was carried out in Swagelok TM cells composed of an Li metal anode, electrolyte (1M LiPF<sub>6</sub> in propylene carbonate (Merck)) impregnated into a glass fiber separator and a porous (13 mm diameter) cathode formed by casting a mixture of Super P carbon (MMM), the appropriate catalyst, and Kynar2801 (a copolymer based on poly(vinylidene fluoride)) in molar ratio 95:2.5:2.5. Cathode construction followed our previously published procedure for porous electrodes.<sup>[8]</sup> The cells were sealed except for the Al grid window that exposed the porous cathode to the 1 atm of O<sub>2</sub> pressure. The Swagelok cells were located within a chamber filled with 1 atm of O<sub>2</sub>, which was itself thermostated at 30 °C. The electrochemical measurements were carried out with a Biologic MacPile cycler.

Received: December 10, 2007

Published online: May 6, 2008

**Keywords:** batteries · energy conversion · lithium · manganese · nanomaterials

- [1] K. Mizushima, P. C. Jones, P. J. Wiseman, J. B. Goodenough, *Mater. Res. Bull.* **1980**, *15*, 783–789.
- [2] T. Nagaura, K. Tozawa, *Prog. Batteries Sol. Cells* **1990**, *9*, 209.
- [3] J.-M. Tarascon, M. Armand, *Nature* **2001**, *414*, 359–467.
- [4] K. M. Abraham, Z. Jiang, *J. Electrochem. Soc.* **1996**, *143*, 1–5.
- [5] J. Read, *J. Electrochem. Soc.* **2002**, *149*, A1190–A1195.
- [6] J. Read, K. Mutolo, M. Ervin, W. Behl, J. Wolfenstine, A. Driedger, D. Foster, *J. Electrochem. Soc.* **2003**, *150*, A1351–A1356.
- [7] T. Kuboki, T. Okuyama, T. Ohsaki, N. Takami, *J. Power Sources* **2005**, *146*, 766–769.
- [8] T. Ogasawara, A. Débart, M. Holzapfel, P. Novák, P. G. Bruce, *J. Am. Chem. Soc.* **2006**, *128*, 1390–1393.
- [9] A. Débart, J. Bao, G. Armstrong, P. G. Bruce, *J. Power Sources* **2008**, DOI: 10.1016/j.jpowsour.2007.06.180.
- [10] C. S. Johnson, D. W. Dees, M. F. Manuette, M. M. Thackeray, D. R. Vissers, D. Argyriou, C.-K. Loong, L. Christensen, *J. Power Sources* **1997**, *68*, 570–577.
- [11] D. Larcher, P. Courjal, R. Herrera Urbina, B. Gérard, A. Blyr, A. du Pasquier, J. M. Tarascon, *J. Electrochem. Soc.* **1998**, *145*, 3392.
- [12] Y. Gao, G. Wang, J. Wan, G. Zou, Y. Qian, *J. Cryst. Growth* **2005**, *279*, 415.
- [13] Synthesis (A. R. Armstrong, P. G. Bruce, to be published): Nanowire  $\beta$ -MnO<sub>2</sub> was prepared by dissolving 1.352 g of MnSO<sub>4</sub>·H<sub>2</sub>O in 40 mL of distilled water and then adding 1.905 g of Na<sub>2</sub>S<sub>2</sub>O<sub>8</sub> to the solution, which was stirred before being transferred to a 40-mL autoclave and heated at 140 °C for 12 h. The resulting product was collected by filtration, washed with distilled water, then ethanol, and dried overnight at 80 °C.
- [14] R. Patrice, PhD thesis, Université de Picardie Jules Verne, **2001**.
- [15] J. Hunter, *J. Solid State Chem.* **1981**, *39*, 142–147.